

Magnetic structure and crystal-field levels in PrAg[†]

T. O. Brun, G. H. Lander, D. L. Price, G. P. Felcher, and J. F. Reddy

Argonne National Laboratory, Argonne, Illinois 60439

(Received 14 June 1973)

Neutron scattering experiments have been performed on polycrystalline samples of PrAg (CsCl structure) to determine the magnetic structure at low temperature and the energy separation of the crystal-field levels. At 14°K PrAg becomes antiferromagnetic with the ($\pi\pi 0$) structure. This consists of ferromagnetic (110) planes coupled antiferromagnetically. Ordered moments of $(2.1 \pm 0.1)\mu_B$ /(Pr atom) lie in the (001) planes. The crystal-field energy levels in PrAg have been measured directly with neutron spectroscopy at 5, 78, and 297°K. The measurements indicate that the Γ_5 level is the ground state. The over-all splitting is ~ 20 meV and the crystal-field parameters W and x are -0.37 ± 0.02 meV and -1.00 ± 0.01 , respectively. A calculation based on a first- and second-neighbor point-charge model with neutral Ag ions and tripositive Pr ions gives reasonable agreement with the experimental parameters. The linewidths of the crystal-field transitions are observed to be very broad (full widths at half-maximum are ~ 11 meV at 297°K). A simple Ruderman-Kittel-Kasuya-Yosida (RKKY) model has been used to explain these widths, which are at least a factor of 2 larger than observed, for example, in the praseodymium monopnictides.

INTRODUCTION

The crystal-field levels in a number of metallic rare-earth monopnictides and chalcogenides have recently been determined successfully by neutron spectroscopy.¹⁻⁶ Rather surprisingly, the level schemes for these compounds, all with the NaCl crystal structure, appear to be consistent with a nearest-neighbor point-charge model if a negative charge is assigned to the nonmetal ion. Such models for the crystal-field levels are usually applied to ionic materials only, and would be expected to have little relevance in metallic systems. To examine further this point we have studied the inelastic neutron scattering from polycrystalline samples of PrAg, which has the CsCl structure. Similar inelastic-neutron-scattering experiments on the rare-earth-Al₂ compounds have been reported,^{7,8} but no details have been given on the widths of the crystal-field transitions, which are one of the most interesting features of the present experiment. Other related experiments are the measurements of the magnetic exciton spectra in singlet-ground-state systems.^{9,10}

The intermetallic compound PrAg has the cubic CsCl structure with a lattice constant $a = 3.739$ Å. This structure is common to almost all the rare-earth intermetallic compounds¹¹ of the form RX , where R is a lanthanide metal and $X = \text{Cu, Ag, or Au}$. Magnetization measurements^{12,13} on PrAg and CeAg have been interpreted as indicating ferromagnetic behavior, with Curie temperatures of 14 and 9°K, respectively. We have found no references to neutron-diffraction experiments on these compounds. A number of other RX compounds have been examined by both bulk magnetization measurements^{12,13} and neutron diffraction.¹⁴⁻¹⁷ All of these compounds are antiferromagnetic.

In the present experiment we measured the inelastic neutron scattering from PrAg at 5, 78, and 297°K, and also determined the magnetic structure in zero magnetic field by neutron diffraction.

EXPERIMENTAL

Sample preparation

The compound PrAg was prepared by arc melting together stoichiometric amounts of the pure elements, and annealing at 700°C for 4 h. Two buttons, each weighing approximately 10 g and measuring 20 mm in diameter by 4 to 5 mm thick, were used for the inelastic-neutron-scattering experiment. For the elastic-neutron-diffraction experiment a powder sample was produced by filing 2 g off one of the buttons, and reannealing. Both the neutron-diffraction and x-ray powder patterns indicated a single-phase cubic material with a lattice parameter of $a = 3.737$ Å, in agreement with the value of 3.739 Å tabulated by Taylor.¹¹ Since PrAg, like most other praseodymium compounds, oxidizes rapidly, the samples were prepared in high-purity argon and sealed in the sample containers before being removed from the inert environment.

Magnetic structure

The powder sample was contained in a thin-walled Al cylinder, $\frac{1}{4}$ -in. diameter, and mounted in a variable-temperature cryostat. The neutron-diffraction patterns were obtained with a conventional two-axis diffractometer located at the CP-5 Research Reactor and using an incident-neutron wavelength of 1.06 Å. Measurements were performed at 78°K, and at several temperatures between 5 and 16°K in zero magnetic field. The diffraction patterns obtained at 5 and 78°K are shown in Fig. 1. The peaks in the 78°K pattern can all be indexed

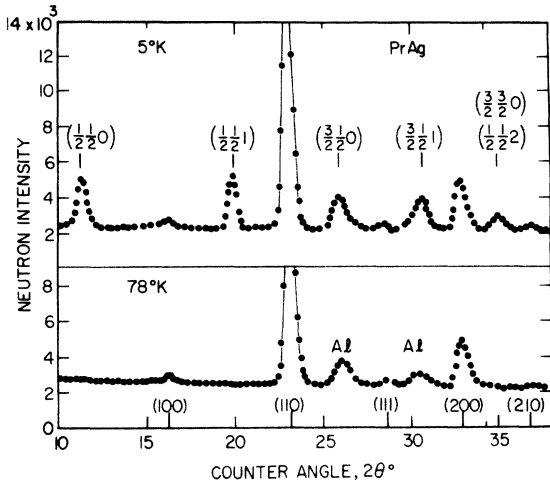


FIG. 1. Neutron-diffraction patterns from a polycrystalline sample of PrAg at 5 and 78 °K.

on the basis of a CsCl crystal structure, and the integrated intensities are in agreement with those calculated using scattering lengths of 0.44 and 0.60 ($\times 10^{-12}$ cm) for Pr and Ag, respectively.¹⁸ At 5 °K additional peaks are observed and the nuclear peaks remain unchanged. This indicates that PrAg is antiferromagnetic at low temperature, and not ferromagnetic as stated in Refs. 12 and 13. The indexing of the magnetic reflections indicates that the magnetic unit cell requires a doubling of the chemical unit cell in the a and b directions. The magnetic structure consists of ferromagnetic (110) planes coupled antiferromagnetically. This structure is the so-called $(\pi\pi 0)$ structure¹⁹ that has been observed in other RX compounds.¹⁴⁻¹⁷ In PrAg the magnetic moments lie in the (001) plane, as determined by the relative intensities of the magnetic peaks. The magnitude of the ordered moment at 5 °K is $(2.1 \pm 0.1) \mu_B$ /(Pr atom). The temperature dependence of the $(\frac{1}{2} \frac{1}{2} 0)$ reflections shows that the Néel temperature is $(14 \pm 1)^\circ\text{K}$. A diffraction pattern obtained at 16 °K shows no evidence for short-range order.

Crystal-field measurements

The two polycrystalline buttons of PrAg were placed in a thin-walled Al container mounted in a fixed-temperature cryostat. The inelastic-neutron-scattering experiment was performed using the "hybrid" neutron spectrometer²⁰ at the CP-5 Research Reactor. This spectrometer consists of a double-crystal monochromator combined with a Fermi chopper for producing the incident beam, and a multiple-detector time-of-flight system for analyzing the energy and momentum transfers of the scattered beam. The incident energy and the burst

time in this experiment were 33.0 meV and 6.7 μsec , respectively. The time of flight of scattered neutrons was measured independently by 15 subgroups of detectors covering scattering angles φ from 14° to 82° . For each subgroup (or scattering angle) the measured time of flight corresponded to an energy transfer of the scattered neutrons between +198 and -21 meV. Measurements were performed with the sample at 5, 78, and 297 °K. Some of the spectra for the large scattering angles contained strong Bragg reflections and also one-phonon coherent peaks from the sample, and these subgroups were not used in the analysis of the crystal-field transitions. For each temperature the time-of-flight spectra in the first eight subgroups (corresponding to $14^\circ < \varphi < 42^\circ$) were found to be identical within counting statistics. The number of scattered neutrons detected for a given energy transfer was therefore summed over the first eight subgroups. The resultant time-of-flight spectra are shown in Fig. 2. (Only the central parts of the spectra are shown in Fig. 2.) The background level due to fast neutrons was measured separately for each subgroup, and the result is in agreement with the number of neutrons detected at large energy transfer in the time-of-flight spectra. This level is indicated by arrows in Fig. 2.

In the interpretation of the time-of-flight spectra the $4f$ -electron configuration of the Pr atoms in PrAg will be assumed to be the $4f^2$ configuration of the tripositive Pr ion. For the free Pr^{3+} ion the 3H_4 ground-state multiplet is separated from the first excited multiplet (3H_5) by ~ 250 meV, so in the crystal-field analysis only the ground state will be considered. In the case of Pr^{3+} the cubic crystal field splits the 3H_4 multiplet into four levels, a singlet Γ_1 and a doublet Γ_3 , both of which are nonmagnetic, and two magnetic triplets Γ_5 and Γ_4 .²¹

In the dipole approximation the differential cross section for paramagnetic scattering of neutrons from a system of noninteracting rare-earth ions in a cubic crystal field is given by

$$\frac{d^2\sigma}{d\Omega d\hbar\omega} \propto [g_J f(\vec{Q})]^2 \frac{k}{k_0} \sum_{i,j} \rho_i \times \sum_{\nu_i, \nu_j} |\langle \Gamma_i \nu_i | J_x | \Gamma_j \nu_j \rangle|^2 \delta(E_i - E_j - \hbar\omega), \quad (1)$$

where k_0 and k are the wave vectors of the incident and scattered neutrons, respectively. The energy gained by the scattered neutrons is $\hbar\omega$. The magnetic form factor $f(\vec{Q})$ is a function of the momentum transfer \vec{Q} . The Landé factor for the J multiplet is g_J , and the Boltzmann factor for the i th crystal-field level is ρ_i . In the matrix elements $\sum_{\nu_i, \nu_j} |\langle \Gamma_i \nu_i | J_x | \Gamma_j \nu_j \rangle|^2$, ν_i and ν_j are indices for the eigenvectors belonging to the representations Γ_i and Γ_j . The transition probabilities have been

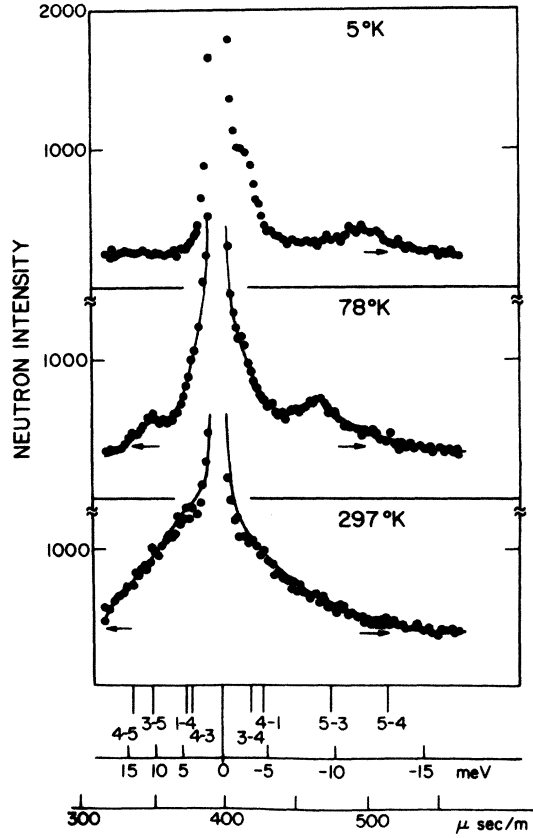


FIG. 2. Inelastic-neutron-scattering spectra from PrAg at 5, 78, and 297 °K. The solid lines are the least-squares fits described in the text. The horizontal arrows are the measured background levels. Below the figure the energies of the crystal-field transitions are indicated, as well as the time-of-flight scale.

tabulated by Birgeneau,²² and for the 3H_4 multiplet only four inelastic transitions, $\Gamma_1-\Gamma_4$, $\Gamma_3-\Gamma_4$, $\Gamma_3-\Gamma_5$, and $\Gamma_4-\Gamma_5$, and two elastic transitions, $\Gamma_4-\Gamma_4$ and $\Gamma_5-\Gamma_5$, are allowed. The dipole approximation is valid only in the limit of $Q \rightarrow 0$; but the corrections²³ to the approximation are very small for the range of momentum transfer ($1.0 < Q < 3.2 \text{ \AA}^{-1}$) in the present experiment, and they have been neglected. Equation (1) makes no allowance for the cross section arising from inelastic scattering by phonons. The phonon cross section for polycrystalline samples increases with increasing momentum transfer Q and energy, and would be expected to exhibit a quite different temperature behavior than that of the inelastic paramagnetic scattering. As discussed above, over the low- Q range we have observed no Q dependence in the scattering, and the over-all temperature dependence is well accounted for by Eq. (1) (see below). Accordingly, we have assumed that the phonon scattering is neg-

ligible in the data presented in Fig. 2. Turberfield *et al.*² established the validity of this assumption in their study of the praseodymium monopnictides and monochalcogenides, and we can expect it to be valid in this case also. A further modification of Eq. (1) is required because the δ -function nature of the crystal-field transitions is not observed in practice. Thus, if the Pr atoms were truly non-interacting the widths of the observed peaks should be comparable to the instrumental resolution, in this case a full width at half-maximum of ~ 1.2 meV. The spectra of Fig. 2 indicate clearly that the crystal-field transitions cannot be described as δ functions, and we have arbitrarily replaced $\delta(E_i - E_j - \hbar\omega)$ in Eq. (1) with the Gaussian function $\exp\{-4 \ln 2 [(E_i - E_j - \hbar\omega)/\sigma_{ij}]^2\}$, where σ_{ij} represents the full width at half-maximum of a transition between the i th and j th levels.

To analyze the data a least-squares program was written to fit the time-of-flight spectra of Fig. 2. The contribution from the paramagnetic scattering was obtained using Eq. (1) with a Gaussian function substituted for the δ function. The crystal-field energy levels E_i , which are contained in the arguments of the Gaussian functions as well as in the Boltzmann factor, were calculated as functions of the parameters W and x defined by Lea, Leask, and Wolf.²¹ The values of the matrix elements were obtained from Ref. 22. The central peak in the spectra was constructed from two Gaussian functions, one representing the quasielastic scattering from the $\Gamma_5-\Gamma_5$ and $\Gamma_4-\Gamma_4$ transitions, and one representing the nuclear elastic scattering from the sample and container. The width of the latter Gaussian is defined by the energy resolution of the instrument. The intensity calculated as a function of neutron energy transfer was converted into energy per time channel, and instrumental corrections for counter efficiency were included. Because of the irregular shape of the samples, no attempt was made in this experiment to reduce the data to absolute differential cross sections. To completely specify the scattering the background level was taken as fixed (see above), and two over-all scale factors, one for the magnetic scattering and one for the nuclear incoherent scattering, were included. In summary, therefore, the parameters for the magnetic scattering are the scale factors, W and x defining the crystal-field levels, and the widths σ_{ij} of the elastic ($i=j$) and inelastic ($i \neq j$) transitions. The spectra at 78 and 297 °K were fitted separately and the results are given in Table I. The function χ^2 is defined by

$$\chi^2 = \left[\sum_{i=1}^N \frac{(\Gamma_i^{\text{obs}} - \Gamma_i^{\text{calc}})^2}{(\delta \Gamma_i^{\text{obs}})^2} \right] / (N - M), \quad (2)$$

where Γ_i^{obs} is the number of neutrons detected in the

TABLE I. Crystal-field parameters determined for PrAg at 78 and 297 °K. W and x are the usual Lea, Leask, and Wolf (Ref. 21) parameters related to the strength of the crystal field and the ratio of the fourth- to sixth-order anisotropy, respectively. The observed widths of the crystal-field transitions are defined by Gaussian functions in the text. For the 78 °K data, widths for magnetic-magnetic transitions σ_{mm} and for nonmagnetic-magnetic transitions σ_{nm} are used. These have been set equal at 297 °K. χ^2 is defined by Eq. (2). The errors quoted in the table and in the text have been obtained directly from the least-squares fitting program using counting statistics. In view of the limitations of Eq. (1) discussed in the text these errors should be treated with caution.

	78 °K	297 °K
W (meV)	-0.328 ± 0.003	-0.37 ± 0.02
x	-0.970 ± 0.002	-1.00 ± 0.01
σ_{mm} (meV)	4.6 ± 0.1	
σ_{nm} (meV)	1.9 ± 0.3	10.9 ± 0.9
χ^2	2.1	1.8

i th time channel, I_i^{calc} is the corresponding calculated count, δI_i^{obs} is the uncertainty in I_i^{obs} , here taken as simply the square root of the observed count, N is the number of time channels considered, and M is the number of parameters. The solid lines in Fig. 2 correspond to the calculated intensity using the parameters of Table I. For the 78 °K data two crystal-field widths σ_{ij} were used, one for the transitions between magnetic levels Γ_5 - Γ_5 , Γ_4 - Γ_4 , and Γ_5 - Γ_4 , and the other for transitions between magnetic and nonmagnetic levels. Only one over-all width was used in analyzing the 297 °K data. The low values of χ^2 for the two temperatures indicate that the introduction of additional width parameters would have little physical significance. At both temperatures the width and position of the central nuclear peak is in agreement with that obtained from a calibration with a vanadium sample.

The agreement between the two sets of values for W and x , determined independently at each temperature, is surprisingly good considering that the spectrum observed at 297 °K has no structure. In the analysis of the 78 °K data we have found that an alternative set of values of W and x (-0.43 meV and -0.8 , respectively) results in a value of χ^2 almost as low as in Table I. The relative positions of the crystal-field energy levels for the two models that fit the 78 °K data are given in Fig. 3. The major difference between the two models is the position of the Γ_3 level with respect to the Γ_5 ground state. However, at 297 °K the values $W = -0.43$ meV and $x = -0.8$ result in a χ^2 of ~ 10 , a value significantly larger than the minimum given in Table I.

Finally we consider the analysis of the spectrum

taken at 5 °K, at which temperature PrAg is ordered antiferromagnetically with a moment of $(2.1 \pm 0.1)\mu_B/(\text{Pr atom})$. Two immediate consequences stem from the fact that the material is ordered magnetically. First, Eq. (1) is invalid since it applies to the paramagnetic phase only; second, we would anticipate a contribution from the spin waves to the inelastic scattering. However, a number of qualitative remarks can be made about the 5 °K spectrum. On the energy-gain side we should not expect to see any crystal-field transitions, since the Γ_5 ground state is the only state populated (see Fig. 3), and neutrons cannot gain energy by deexciting the system. Figure 2 indicates that this is indeed the case. The transitions expected on the energy-loss side must involve the Γ_5 ground state, and are therefore Γ_5 - Γ_3 and Γ_5 - Γ_4 . The transition at ~ -12 meV in Fig. 2 may correspond to a combination of these two transitions, but in the model presented in Table I (left-hand side of Fig. 3) no transition involving Γ_5 can account for the shoulder observed at ~ -3 meV. The alternative model ($W = -0.43$ meV, $x = -0.8$) would account for both features of the spectrum; but, in view of the qualitative nature of this discussion, this assignment of the crystal-field transitions should be regarded with caution.

DISCUSSION

The crystal-field Hamiltonian for a trivalent rare-earth ion can be written as

$$H_c = A_4 \langle r^4 \rangle \beta O_4 + A_6 \langle r^6 \rangle \gamma O_6 \quad (3)$$

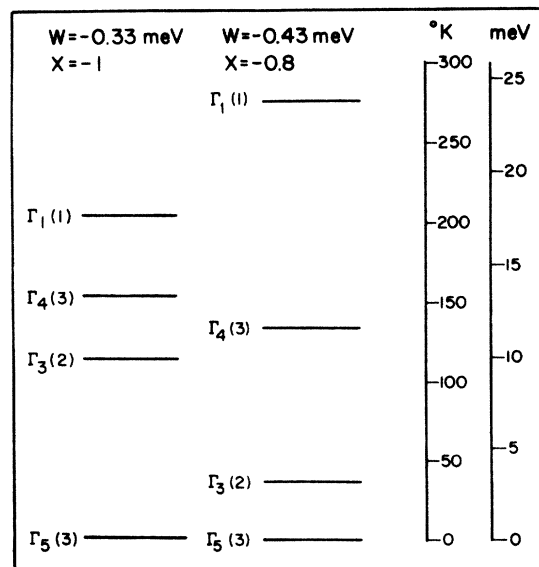


FIG. 3. Models for the crystal-field levels of the Pr^{3+} ion in PrAg.

in terms of the Stevens operator equivalents O_4 and O_6 . The remainder of the terms in Eq. (3) are defined in Lea, Leask, and Wolf.²¹ Pierre¹⁵ analyzed his magnetization data for CeAg in terms of a Hamiltonian including both the crystal-field and exchange interactions and concluded that the geometrical coefficient A_4 is negative for CeAg. Assuming the coefficient A_4 does not vary much throughout the rare-earth series, Pierre predicted that the ground state of the Pr^{3+} ion in PrAg would be Γ_5 . This agrees with the crystal-field level scheme that we have derived from our inelastic-neutron-scattering experiment. Furthermore, the saturation moment of the Γ_5 ground state is $2\mu_B$, in good agreement with the value of $(2.1 \pm 0.1)\mu_B$ obtained from the powder diffraction experiment at 5 °K.

The experimental values for $A_4\langle r^4 \rangle$ and $A_6\langle r^6 \rangle$ can be calculated from the values of W and x given in Table I. Using the results obtained at 78 °K,

$$A_4\langle r^4 \rangle = -7.21 \pm 0.06 \text{ meV}$$

and

$$A_6\langle r^6 \rangle = -0.0128 \pm 0.0006 \text{ meV}, \quad (4)$$

Pierre¹⁵ deduced from the results for CeAg that the splitting between the Γ_8 ground state and the Γ_7 excited state is 31 meV, which leads to a value of -13.5 meV for $A_4\langle r^4 \rangle$. Using the values for $\langle r^n \rangle$ integrals calculated by Freeman and Watson,²⁴ and assuming A_4 constant, the results for CeAg predict that $A_4\langle r^4 \rangle$ for PrAg should be between -10 and -11 meV, in reasonable agreement with the present experimental result.

The observed values for $A_4\langle r^4 \rangle$ and $A_6\langle r^6 \rangle$ can also be compared to calculations using a simple point-charge model, which is successful in the praseodymium monopnictides and monochalcogenides.² In these materials with the NaCl crystal structure the experimental values for W and x could be reproduced if an effective charge of $-2|e|$ was assigned to the octahedrally coordinated anions. The value of x found for PrAg is very close to that observed for the pnictides and chalcogenides, but W has the opposite sign. In terms of a point-charge model, this indicates that the crystal-field interactions in PrAg could arise from a set of octahedrally coordinated *positive* charges. If the charge on the nearest neighbors, Ag with cubic environment, is zero, and the next nearest neighbors, Pr with octahedral environment, are considered tripositive, then $A_4\langle r^4 \rangle$ and $A_6\langle r^6 \rangle$ are -5.8 and -0.07 meV, respectively. These values compare surprisingly well with the experimental values in Eq. (4).

Another intermetallic compound in which the non-rare-earth ion appears to have zero effective charge is YbPd_3 , as shown by a recent Mössbauer experi-

ment.²⁵ In this, the point-charge model appears to explain the crystal-field levels if, as in PrAg, the nearest-neighbor atoms (in this case Pd) are assumed to be neutral. On the other hand, experiments on dilute rare-earth impurities in noble metals²⁶ indicate that the sign of $A_4\langle r^4 \rangle$ is opposite to that expected with a point-charge models. We believe an understanding of whether or not the agreement with the point-charge model in many of these materials is fortuitous must await further experiment and theory.

One of the most interesting features of our study of PrAg is the widths, and their temperature dependence, of the crystal-field transitions. The paramagnetic cross section used here [Eq. (1)] has been used previously,²⁻⁵ but the widths of the crystal-field transitions are at least a factor of 2 greater than other reported values at similar temperatures. For example, comparable values in PrS_2 are 5.4 meV, and in NdP,⁴ 3.1 meV. At 297 °K the widths in PrAg are comparable to the spacings between the crystal-field levels themselves, and, under these conditions, we should not expect Eq. (1) to be valid, although the low value of χ^2 in Table I indicates a good fit. A more realistic cross section that includes the effects of various interactions between the rare-earth ions, as well as the crystal field, should be derived theoretically. The result of combining exchange interactions and single-ion anisotropy effects has been considered,²⁷ but no detailed cross section has been published.

Perhaps the most obvious contribution to the line broadening is from the exchange interactions, although it is noteworthy that the neodymium pnictides,⁴ for example, have narrower crystal-field transitions but higher ordering temperatures. If single-ion anisotropy effects are neglected, and the exchange interactions are known, the second moment $\langle \hbar^2 \omega^2 \rangle$ of the quasielastic scattering from a paramagnetic powder can be calculated.²⁸ At high temperature and for large scattering angles, the shape of the quasielastic peak is approximately Gaussian, and the second moment of the peak is given by

$$\langle \hbar^2 \omega^2 \rangle = \sum_l \frac{2}{3} J(J+1) \mathcal{J}_l^2, \quad (5)$$

where \mathcal{J}_l is the exchange for the l th neighbor. For PrAg two parameters, the Néel temperature T_N and the paramagnetic Curie temperature Θ_p , are available for determining \mathcal{J}_l . In a molecular-field model, for which only first and second nearest neighbors are considered,²⁹ \mathcal{J}_1 and \mathcal{J}_2 cannot be determined independently for the $(\pi\pi 0)$ antiferromagnetic structure, since this structure imposes the relationship $|\Theta_p| = 3T_N$. An alternative model having only two parameters is the free-electron Ruderman-Kittel-Kasuya-Yosida (RKKY) interaction

model discussed by Pierre¹⁵ and Sears.³⁰ Assuming that the $(\pi\pi 0)$ structure is stable, and using $\Theta_p = 2^\circ\text{K}$ ¹² and $T_N = 14^\circ\text{K}$, the second moment given by Eq. (5) is $\sim 3.7\text{ meV}^2$. This value corresponds to a full width at half-maximum of $\sim 4\text{ meV}$, which is similar in magnitude to the values in Table I. The simple RKKY model also predicts that the exchange interactions in PrAg almost favor ferromagnetism. This may explain the magnetization measurements of Pierre and Pauthenet,¹³ who reported PrAg to be ferromagnetic. Considering the simplicity of the free-electron RKKY model and the exclusion of crystal-field interactions in the

derivation of the exchange interactions, the reasonable agreement with the experimental data indicate that the large widths of the crystal-field transitions in PrAg could probably be accounted for by the long-range and oscillatory nature of the indirect exchange through the conduction electrons.

ACKNOWLEDGMENTS

We would like to thank R. Kleb and G. E. Ostrowski for experimental assistance, and B. D. Dunlap and B. R. Cooper for a number of helpful discussions.

[†]Work performed under the auspices of the U. S. Atomic Energy Commission.

¹B. D. Rainford, K. C. Turberfield, G. Busch, and O. Vogt, *J. Phys. C* **1**, 679 (1968).

²K. C. Turberfield, L. Passell, R. J. Birgeneau, and E. Bucher, *Phys. Rev. Lett.* **25**, 752 (1970); *J. Appl. Phys.* **42**, 1746 (1971).

³R. J. Birgeneau, E. Bucher, L. Passell, and K. C. Turberfield, *Phys. Rev. B* **4**, 718 (1971).

⁴A. Furrer, J. Kjems, and O. Vogt, *J. Phys. C* **5**, 2246 (1972).

⁵A. Furrer, W. Buhner, H. Heer, W. Halg, J. Benes, and O. Vogt, in *Proceedings of the International Symposium on Neutron Inelastic Scattering, Grenoble, 1972* (I. A. E. A., Vienna, 1973), p. 563.

⁶H. L. Davis and H. A. Mook, *AIP Conf. Proc.* **10**, 1548 (1973).

⁷H. G. Purwins, E. Walker, P. Donze, A. Treyvand, A. Furrer, W. Buhner, and H. Heer, *Solid State Commun.* **12**, 117 (1973).

⁸A. Furrer, W. Buhner, W. Halg, H. Heer, J. Kjems, H. G. Purwins, and E. Walker, *AIP Conf. Proc.* **10**, 1059 (1973).

⁹B. D. Rainford and J. G. Houmann, *Phys. Rev. Lett.* **26**, 1254 (1971).

¹⁰R. J. Birgeneau, J. Als-Nielsen, and E. Bucher, *Phys. Rev. B* **6**, 2724 (1972).

¹¹K. N. R. Taylor, *Advan. Phys.* **20**, 551 (1971).

¹²R. E. Walline and W. E. Wallace, *J. Chem. Phys.* **41**, 3285 (1964).

¹³J. Pierre and R. Pauthenet, *C. R. Acad. Sci. (Paris)* **260**, 2739 (1965).

¹⁴J. W. Cable, W. C. Koehler, and E. O. Wollan, *Phys.*

Rev. **136**, A240 (1964).

¹⁵J. Pierre, in *Proceedings of the Eighth Rare-Earth Research Conference*, edited by T. A. Henrie and R. E. Lundstrom (Reno Metallurgy Research Center, Reno, Nevada, 1970), p. 102.

¹⁶G. Arnold, N. Nereson, and C. E. Olsen, *J. Chem. Phys.* **46**, 4041 (1967).

¹⁷N. Nereson, *AIP Conf. Proc.* **10**, 669 (1973).

¹⁸Neutron Diffraction Commission, *Acta Crystallogr.* **A 28**, 357 (1972).

¹⁹H. A. Gersch and W. C. Koehler, *J. Phys. Chem. Solids* **5**, 180 (1958).

²⁰R. Kleb, G. E. Ostrowski, D. L. Price, and J. M. Rowe, *Nucl. Instrum. Methods* **106**, 221 (1973).

²¹K. R. Lea, M. J. M. Leask, and W. P. Wolf, *J. Phys. Chem. Solids* **23**, 1381 (1962).

²²R. J. Birgeneau, *J. Phys. Chem. Solids* **33**, 59 (1972).

²³W. Marshall and S. W. Lovesey, *Theory of Thermal Neutron Scattering* (Oxford U. P., Oxford, England, 1971), pp. 169–172.

²⁴A. J. Freeman and R. E. Watson, *Phys. Rev.* **127**, 2058 (1962).

²⁵I. Nowik, B. D. Dunlap, and G. M. Kalvius, *Phys. Rev. B* **6**, 1048 (1972).

²⁶G. Williams and L. L. Hirst, *Phys. Rev.* **185**, 407 (1969).

²⁷See p. 479 in Ref. 23.

²⁸W. Marshall and R. D. Lowde, *Rep. Prog. Phys.* **31**, 705 (1968).

²⁹D. ter Haar and M. E. Lines, *Philos. Trans. R. Soc. Lond. A* **254**, 521 (1962).

³⁰V. F. Sears, *Can. J. Phys.* **45**, 2923 (1967).